Elsevier Editorial System(tm) for Journal of Structural Geology
Manuscript Draft

Manuscript Number: SG-D-09-00044R2

Title: Visualizing Strain and the Rf-Φ Method with an Interactive Computer Program

Article Type: Original Research Article

Keywords: strain analysis; Rf-Φ method; computer program; conglomerate

Corresponding Author: Professor Paul Karabinos, Ph.D.

Corresponding Author's Institution: Williams College

First Author: Paul Karabinos

Order of Authors: Paul Karabinos; Paul Karabinos, Ph.D.; Chris Warren

Abstract: The Rf-Φ method is a powerful graphical approach for estimating finite strain of deformed elliptical objects, but one that students commonly find difficult to understand. We developed a program that allows users to explore visually how deforming a set of elliptical objects appears on Rf-Φ plots. A user creates or loads the ellipses and then deforms them by simple shear, pure shear, or rigid rotation. As the ratio of the long to short axis of the ellipses (Rf) and long-axis orientations (Φ) change in one window, the Rf-Φ plot continuously and instantaneously updates in another. Users can save snapshots of the deformed elliptical objects and the Rf-Φ plots to record graphical experiments. The program provides both Rf vs. Φ and polar ln(Rf) vs. 2(Φ) plots. The user can 'undeform' ellipses quickly and easily, making it possible to inspect the 'original' shapes and orientations of objects, and to evaluate the plausibility of the determined strain values. Users can export information about the pebbles' shape and orientation to spreadsheets for rigorous statistical analysis. This program is written in Java and so can run on virtually any operating system. Both the source code and the application will be freely available for academic purposes.

***Revision Notes**

September 1, 2009

Dear Bill:

Thanks very much for your great editorial suggestions. I have incorporated all of them with a few minor adjustments.

Sincerely,

Paul Karabinos

Visualizing Strain and the R_f-Φ Method with an Interactive Computer Program

Paul Karabinos
Department of Geosciences
Williams College
Williamstown, MA 01267,
Corresponding author, tel: 413.597.2079; fax: 413.597.4116;
email: pkarabin@williams.edu
and

Chris Warren
Office of Information Technology
Williams College
Williamstown, MA 01267

Abstract

The R_f-Φ method is a powerful graphical approach for estimating finite strain of deformed elliptical objects, but one that students commonly find difficult to understand. We developed a program that allows users to explore visually how deforming a set of elliptical objects appears on R_f-Φ plots. A user creates or loads the ellipses and then deforms them by simple shear, pure shear, or rigid rotation. As the ratio of the long to short axis of the ellipses (R_f) and long-axis orientations (Φ) change in one window, the R_f-Φ plot *continuously and instantaneously* updates in another. Users can save snapshots of the deformed elliptical objects and the R_f-Φ plots to record graphical experiments. The program provides both R_f vs. Φ and polar ln(R_f) vs. 2(Φ) plots. The user can 'undeform' ellipses quickly and easily, making it possible to inspect the 'original' shapes and orientations of objects, and to evaluate the plausibility of the determined strain values. Users can export information about the pebbles' shape and orientation to spreadsheets for rigorous statistical analysis. This program is written in Java and so can run on virtually any operating system. Both the source code and the application will be freely available for academic purposes.

Keywords: strain analysis, R_f-Φ method, computer program, conglomerate

1. Introduction

Deformed ellipsoidal objects, such as pebbles and oolites, are common in rocks, and they offer an intuitive, visually appealing approach for teaching fundamental strain concepts in structural geology. Students can easily grasp the effect of strain on an initially spherical object and, with practice, can visualize the fate of initially ellipsoidal markers. Furthermore, the study of deformed pebble conglomerate and oolitic limestone provides an excellent opportunity for students to gain experience in data acquisition and error analysis. They must also confront a host of important problems that plague all attempts to quantify strain, such as ductility contrast between marker object and matrix, initial shape and distribution of marker objects, area or volume change during deformation, and the

relationship between two-dimensional strain measured in planar sections with the three-dimensional strain experienced by rocks.

Structural geologists commonly exploit elliptical objects in their research to quantify strain in naturally deformed rocks, understand the development of deformation fabrics, and examine strain gradients in folds and fault zones. The importance of this approach to strain measurement has inspired numerous studies to overcome its inherent limitations, or at least to understand them thoroughly. Through numerical experiments, Lisle (1979) tested several methods for averaging shape and orientation data to determine the most accurate for estimating the strain ellipse, and concluded that the harmonic mean was the most reliable. Hossack (1968) and Treagus and Treagus (2002) also discussed in detail the problems of determining strain from pebble shapes in a conglomerate.

Ramsay (1967) derived the equations of the R_f-Φ method for quantifying finite strain, and Dunnet (1969) showed how the R_f-Φ method can be used as a practical tool for strain determination from elliptical objects. As discussed in detail below, the R_f-Φ method assumes an initially random distribution of ellipse long-axis orientations, and a range of initial long to short axial ratios, R_i (Table 1). Ramsay and Huber (1983) presented an especially useful, and well-illustrated, discussion of the R_f-Φ method making the technique more accessible to researchers and students. Lisle (1985) offered a very complete and useful treatment of the method. Our contribution is to provide a program that links deformation of elliptical objects with R_f-Φ plots, giving students a *visual* explanation of how the method works, and offering students and researchers a tool to quickly estimate strain from outcrops and samples.

Our program provides both the familiar Cartesian R_f-Φ plot and the innovative polar plot of Elliott (1970) for comparison with the ellipse population. Elliott's (1970) approach employed a novel "shape factor grid" and a polar plot of $\ln(R_f)$ vs. $2(\Phi)$ that should, in theory, allow assessment of the initial distribution of long axes of elliptical objects, and estimate the strain. The greatest limitation of this approach is the apparent complexity of the distribution of undeformed elliptical objects (Boulter, 1976; Paterson and Yu, 1994). Yamaji (2005) developed an inverse method to overcome some of these limitations for the special case of a bivariate normal distribution of sedimentary particles. Another limitation to Elliott's (1970) approach, and a possible explanation for why the

method has been underutilized, is the significant difficulty most users have with visualizing the effect of strain on elliptical objects in polar plots. Our program helps overcome the latter limitation by showing how Cartesian and polar R_f-Φ plots change during deformation.

Lisle's (1985) approach to testing the assumption of an initially random distribution of pebble long axes was to create a set of "marker deformation grids" using Cartesian R_f-Φ plots, and to examine the distribution pattern of deformed ellipses. Sets of pebbles that were consistent with the assumption should show a symmetrical pattern about both the harmonic mean of R_f and the vector mean of Φ. DePaor (1988) developed another novel and useful approach to the R_f-Φ method that uses a hyperbolic net and symmetry principles to estimate strain from ellipsoids, but our program does not include hyperbolic plots.

Several commercially available drafting programs allow users to create a set of elliptical objects and to simulate deformation with tools that linearly transform the ellipses by pure shear, simple shear, and rigid rotation. These programs are very useful for teaching purposes. Also, several commercial programs are available that permit researcher to determine strain with the R_f-Φ method using axial ratio and orientation data. Some of these programs incorporate statistical methods to assess the validity of the assumption of initial random distribution of long axis orientations. We have not duplicated the capabilities of these programs. Instead, we developed a relatively simple program that focuses on *visualizing* the relationship between strained elliptical objects and plots of axial ratio vs. orientation. Our program is complimentary to the existing software because it is straightforward to examine deformed objects with our program and then, to export information about the ellipses to data files for use in these programs.

Our goal was to create a simple and easy-to-learn interactive computer program that allows the user to simulate deformation of elliptical objects by pure shear, simple shear, and rigid rotation. Throughout the linear transformations, Cartesian or polar R_f-Φ plots are continuously and instantaneously updated. The advantage of this program is that the color coding and tracking options make it possible to visualize the distribution *and paths* of points representing elliptical objects on R_f-Φ plots. This is especially valuable for the polar plots of $\ln(R_f)$ vs. $2(\Phi)$, and it helps highlight the potential of this neglected

approach. We also show here how the program is used to introduce students to the R_f-Φ method, determine strain in natural samples, and simulate 'retro-deformation' of samples to recover the original shapes and orientation of the pebbles for critical evaluation of the method. This program is written in Java, and so can run on virtually any operating system. Both the source code and the finished application will be freely available for academic purposes.

2. Summary of the Program

The program contains a large display window on the left and a display control window on the right (Fig. 1A). Ellipses are created in the display area by dragging with the mouse in editing mode. The user can import a 700 by 700 pixel photograph or other image as a background, and trace elliptical objects from it (Fig. 1B). Alternatively, text files containing information about the position, shape, and orientation of elliptical objects can be loaded. An Excel workbook that serves as a template for creating such files is included with the program. Several buttons control the appearance of the ellipses and the scale and position of the display (Table 2). All pebbles in the display area are plotted in the small R_f vs. Φ plot in the display control window as they are created (Fig. 1A).

The user can choose deformation by simple shear, pure shear, or rigid rotation with the radio buttons (Fig. 1). Once a radio button is chosen, deformation can be precisely specified or accomplished by click-and-drag with the mouse in the display area. During simulated deformation, the R_f vs. Φ plot is continuously and instantaneously updated as ellipses change shape and orientation in the display area. A larger and more versatile R_f vs. Φ plot appears when the user clicks the Big Cartesian Plot button. The Big Polar Plot button summons a polar plot of $\ln(R_f)$ vs. $2(\Phi)$, which tracks deformation of elliptical objects in a different and very useful manner (Elliott, 1970), as discussed below. The program allows the user to save an image of both types of plots.

Original and deformed displays can be saved for further study. Data files containing information about the original or deformed shape, orientation, and position, of pebbles can be created for statistical analysis or use with commercially available programs. Snapshots of the display can be captured, and a sequence of such images, combined with snapshots of the R_f-Φ plots, can be used to create animations of

deforming pebbles and the corresponding changes in the graphical representation of the deformation.

The program applies the specified linear transformation to simulate deformation of ellipses in the display area. The program then uses a simple numerical analysis process to determine the axial ratio of the transformed objects. For each ellipse, it gets a list of points along the circumference, and then calculates the distance from the center to each of those points. As it steps through those calculations, it tracks the longest and shortest of those distances, thus finding the long and short axes. To maximize the accuracy and efficiency of the axial ratio approximation, the program uses a number of circumference points close to the number of pixels used to create the ellipse. The analytical equations for Φ and R_f derived by Ramsay (1967, p. 205-209) and summarized by Lisle (1985, p. 3) can be used to track deforming ellipses, particularly when their shapes and orientations are loaded from a file (e.g. Fig 1A). However, when ellipses are traced from an image (e.g. Fig. 1B), a numerical routine similar to the one we use is needed to determine the initial shape and orientations of objects. The routine we use mimics what geologist actually do when they measure naturally deformed elliptical objects.

3. Demonstrating the R_f-Φ Method to Students

Figure 2A shows five color-coded groups of ellipses from the display screen with initial axial ratios equal to 1.2, 1.6, 2.0, 2.4, and 2.8. The long axes of the ellipses are initially oriented in 10^o increments. We created this group of ellipses as a teaching aid using the Excel Workbook distributed with the program. It is designed to simulate a group of pebbles with an initially random distribution of long axis orientations, and a limited range of axial ratios. Figure 2B shows the R_f vs. Φ plot for this 'undeformed' array of ellipses. The points are colored the same as the corresponding ellipses, to facilitate tracking, and they are distributed over the entire range of Φ values. Two ellipses with axial ratios of 2.8, whose long axes are oriented horizontally and vertically are selected in 2A, and they appear as larger points in 2B to highlight the paths of these objects during simulated deformation. Also selected in 2A is the large gray unit circle to help track the value of the "strain ellipse" in the R_f-Φ plots. Figure 2C shows the polar plot of $\ln(R_f)$ vs. $2(\Phi)$ for the undeformed array of ellipses. The points are also colored

the same as the ellipses in 2A, and the points form a radial distribution around the origin of the polar plot with more elliptical objects farther from the origin.

The ellipses undergo a simulated vertical, pure shear, shortening with strain ratio of 1.4 (Fig. 2D). The R_f-Φ plot (Fig. 2E) shows that the ellipses with initial axial ratios of 1.2 now form a closed loop. The polar plot of $\ln(R_f)$ vs. $2(\Phi)$ (Fig. 2F) shows that the points corresponding to the group of ellipses with an initial axial ratio of 1.2 now lie entirely to the right of the origin. This pattern reflects the fact that the strain ($R_s = 1.4$) was great enough to transform an initial ellipse ($R_i = 1.2$), whose long axis was perpendicular to the stretching direction, to a circular object ($R = 1$), and then into an ellipse whose long axis is parallel to the stretching direction ($R_f = 1.17$). In contrast, groups of ellipses with initial axial ratios greater than that of the strain ellipse form open configurations in the R_f-Φ plot over the entire range of Φ values. This pattern reflects the fact that elliptical objects, whose axial ratios are greater than the strain ellipse ratio, and whose long axes are perpendicular to the stretching direction, become less elliptical, but their long axes do not change orientation during pure shear.

Continuing this example, the shortening is increased to a strain ratio of 3:1 (Fig. 2G). At Rs = 3, points representing all the ellipses form concentric closed loops on the R_f vs. Φ plot (fig. 2H) because Rs is greater than the maximum initial ellipticity of 2.8. On the polar plot (fig. 2I), all of the points lie to the right of the origin and together they form a noticeably elliptical, rather than a circular, distribution.

The images in Figure 2 illustrate, in an effective but static fashion, the relationship between the strained elliptical shapes and the Cartesian and polar R_f-Φ plots. Using the program is much more compelling, however, because the R_f-Φ plots are continuously and instantaneously updated as the ellipses are strained in the display window, and the user can rapidly perform experiments that visually relate strain to the plots.

To find the R_f and Φ values for individual objects, the user clicks on the point in the plots and reads the coordinates at the bottom of the window. Thus, it is easy to determine the values of R_{fmax} and R_{fmin} on the R_f vs. Φ plots (Figs. 2E and H), and to use them to calculate the maximum initial ellipticity, R_{imax}, and the axial ratio of the strain ellipse, R_s, using the equations provided by Ramsay and Huber (1983, p. 77). For

example in Figure 2E, $R_{fmax} = 4.1$ and $R_{fmin} = 2.1$. Using these values in the equations for an open configuration:

$$(R_{fmax} * R_{fmin})^{1/2} = R_{imax}, \text{ and} \quad (1)$$

$$(R_{fmax} / R_{fmin})^{1/2} = R_s, \quad (2)$$

yields $R_{imax} = 2.9$, and $R_s = 1.4$. In Figure 2H the maximum and minimum values are 8.9 and 1.1. Using these values in the equations for a closed configuration:

$$(R_{fmax} / R_{fmin})^{1/2} = R_{imax}, \quad (3)$$

$$(R_{fmax} * R_{fmin})^{1/2} = R_s, \quad (4)$$

gives $R_{imax} = 2.8$, and $R_s = 3.1$. Both of these results are in good agreement with the actual values for strain and maximum initial ellipticity used in the simulations.

For an initially random distribution of elliptical objects, finding the R_s value in the polar plots is very straightforward. It requires locating the 'center' of the points representing all of the ellipses and clicking on it. The $\ln(R_f)$ and the R_f values are given at the bottom of the plot. One of the inherent challenges of the R_f-Φ method is identifying outliers (pebbles with unusually large initial ellipticity values) on the R_f vs. Φ plot so that they may be neglected when finding the values of R_{fmax} and R_{fmin} to use in Eqs. (1) and (2) for open configurations or Eqs. (3) and (4) for closed configurations (Ramsay and Huber, 1983). Using the polar plot circumvents this problem by focusing on the *center* of the distribution of points, rather than on the maximum and minimum values. Thus, the correct identification of outliers is much less critical.

Figures 2E and H help illustrate an important limitation of the R_f - Φ method. It is only reliable if the undeformed rock contained a large number of objects that possessed the *greatest* initial axial ratio, R_{imax}, and the long axes of these objects were not preferentially oriented. Both criteria must be met to create a robust open (Fig. 2E) or closed (Fig. 2H) configuration for determining R_{fmax} and R_{fmin}. If only a limited number

of objects with greatest initial ratio are present, or if the long axes are preferentially oriented over a limited angular range, the values for R_{fmax} and R_{fmin} obtained from Cartesian R_f - Φ plots will be based on pebbles with different initial ellipticity (for example, purple and yellow ellipses in Fig. 2). This situation will produce an inaccurate strain estimate. Tracking specific points allows the user to see that after deformation, objects with maximum initial axial ratios ($R_i = R_{imax}$), and with long axes parallel to the maximum extension direction, will have the greatest final axial ratio ($R_{imax} * R_s = R_{fmax}$). In contrast, objects with maximum initial axial ratios (again, $R_i = R_{imax}$), but with long axes perpendicular to the maximum extension direction will have the minimum final axial ratio ($R_{imax}/R_s = R_{fmin}$). If the observed values for R_{fmax} and R_{fmin} come from unique outliers, that is to say, pebbles with significantly different initial ratios, R_i, the strain estimate will not be reliable.

4. Applying the R_f-Φ Method for Strain Determinations

Figure 3A shows the program window with a background image of a deformed quartz pebble conglomerate from the Dalton Formation, located in Dalton, Massachusetts, USA. The photograph was converted into a 700 by 700 pixel image before being loaded as a background. The blue ellipses were traced from the deformed pebbles in the editing mode by clicking and dragging with a mouse. An experienced user can trace fifty pebbles in approximately five minutes, so it is an efficient method for determining the axial ratio and long axis orientation of deformed pebbles, compared with measuring individual pebbles with a ruler and protractor. The ellipses generated by the program rarely conform to the shape of naturally deformed objects. Thus, using the program to trace pebbles highlights the important, yet commonly overlooked, fact that naturally deformed objects are not perfect ellipses. As pebble outlines are traced with a mouse, the corresponding R_f and Φ values are plotted in Cartesian (Fig. 3B) and polar (Fig. 3C) plots.

After the pebbles are traced, the R_f - Φ plot (Fig. 3B) can be used to find the values of R_{fmax} and R_{fmin} (as shown in Figures 2E and H). Once these values are obtained, it is straightforward to calculate the ratio of the strain ellipse, R_s, and the maximum initial

ellipticity, R_{imax}, using Eqs. (1) and (2) for open configurations, or Eqs. (3) and (4) for closed configurations.

Another approach, which offers greater insight into the strain state, is to use the program to find the most likely inverse strain ellipse, and thereby recover the 'undeformed' shapes and distribution of the pebbles. This is most easily done in two steps, and the process takes advantage of the fact that an arbitrary linear transformation can be expressed as a pure shear (transformation by a diagonal matrix) followed by a rotation (transformation by an anti-symmetric matrix). These steps are reversed for an inverse transformation (inverse strain).

Figure 3D shows the pebble outlines after a counter-clockwise rigid rotation of 9^o, a value found by trial and error and chosen because it creates a symmetric distribution of points about the $\Phi = 0$ axis in the R_f vs. Φ plot (Fig. 3E), and the $2\Phi = 0$ axis in the polar $\ln(R_f)$ vs. 2Φ plot (Fig. 3F). The second step is to apply horizontal shortening by pure shear, and create the most dispersed possible distribution of points over the entire range of Φ values (Fig. 3H). A dispersed pattern of points, as seen in Figure 3H, simulates an initially random distribution of long axis orientations. An equivalent approach is to create a radial distribution of points centered at the origin of the polar plot of $\ln(R_f)$ vs. 2Φ to simulate an initially random distribution of long axis orientations (Fig. 3I).

The axial ratio of the inverse strain ellipse determined by the inverse graphical method is 3.7. This strain estimate is similar to the value of Rs = 3.67 as calculated using Eq. (4) with values of $R_{fmin} = 1.95$ and $R_{fmax} = 6.93$, as measured from Figure 3B. Likely outliers were neglected when selecting the R_{fmin} and R_{fmax} values. By comparison, field measurements at the outcrop using a ruler and protractor gave a strain estimate of 3.75 using the standard R_f - Φ method (Ramsay and Huber, 1983). As expected, the agreement between the three approaches is excellent. The inverse graphical strain method, however, has the advantage of allowing visual inspection of the starting configuration of the pebbles. The value of direct field measurements cannot be overstated, and should always be the highest priority. However, it is not always possible to measure objects on inaccessible surfaces in the field, and our program is well suited for working with photographs of hard-to-reach outcrop surfaces, as well as photographs of slabbed hand samples and thin sections.

The graphical approach for finding inverse strain described above is valuable because the initial shapes of the pebbles, and their spatial distribution, can be easily portrayed (Fig. 3G). This functionality makes it possible for researchers and students to assess quickly and *visually* the plausibility of strain determinations using the R_f-Φ method. Furthermore, although the examples presented here assume no area change, the program can incorporate area change if such data are available. Because the program runs graphical experiments very quickly, it is also practical to explore the effects of varying area change if the direction of area loss can be deduced from stylolites or pebble indentations (Onasch, 1984).

5. Conclusions

Although we do not provide new insight into the theory behind the R_f-Φ method, we believe our program advances strain studies for both educational and research purposes. Our main goal in creating this program was to provide a *visual* link between deforming elliptical objects and corresponding R_f-Φ plots, and we endeavored to do this with an easy-to-learn application so attention can be focused on strain rather than learning how to use the program. Instructors can use the main display window to demonstrate fundamental principles of strain, such as the difference between coaxial and non-coaxial strain, and the relationship between strain and deformation fabric. The program also allows students to see how deformation of a group of ellipses is manifested in R_f-Φ plots, and how strain can be estimated from such a population. The digitizing capabilities of the program make it possible for students to quickly generate R_f-Φ plots from photographs of deformed conglomerate or oolitic limestone, making it more practical to assign such problems.

The program generates both the familiar Cartesian R_f-Φ plots and polar plots of $\ln(R_f)$ vs. $2(\Phi)$, as suggested by Elliott (1970). Direct comparison of the two kinds of plots highlights the advantages and disadvantages of each. Although the polar plots are somewhat more difficult to relate to the shape and orientation of elliptical objects, the program demonstrates that the initial array of points representing ellipses is displaced with only moderate distortion in the $\ln(R_f)$ vs. $2(\Phi)$ plots (Figs. 2 & 3). Recognition and

elimination of statistical outliers is also much less critical when using polar than Cartesian plots.

Researchers can use the program to digitize deformed objects from imported photographs of outcrops, slabbed hand samples, and thin sections. Strain can be determined directly from the R_f-Φ plots using the standard equations, or by retro-deformation of the ellipses, as described above. The advantage of the latter approach is that it gives a view of the initial shape and distribution of objects, and thereby permits a visual assessment of the validity of the strain estimate. The program can model area change during deformation, and graphical experiments can be performed rapidly, so it is feasible to explore the effects of area change when evidence for pressure solution exists (Onasch, 1984). The program does not provide automated strain determinations or testing of initially random distribution of ellipses. It is easy, however, to export data files with information about the position, axial ratio, and long axis orientation of ellipses. Such files can then be used for statistical and graphical analysis to test rigorously strain models, and the assumptions on which they are based. Data files generated by our program can also be imported into commercially available programs that perform symmetry and distribution tests on deformed objects.

The program, which we call GeoShear, along with a photograph of a deformed conglomerate, files of synthetic ellipses, and an Excel workbook that serves as a template for creating new files can be downloaded at: http://www.williams.edu/Geoscience/facultypages/Paul/currentresearch.html.

Acknowledgements

We thank Matty Mookerjee, an anonymous reviewer, and William Dunne for valuable suggestions for improving the manuscript.

References

Boulter, C.A., 1976, Sedimentary fabrics and their relation to strain-analysis methods. Geology 4, 141-146.

De Paor, D.G., 1988, R_f/Φ strain analysis using an orientation unit. Journal of Structural Geology 10, 323-333.

Elliott, D., 1970, Determination of finite strain and initial shape from deformed elliptical objects. Geological Society of America Bulletin 81, 2221-2236.

Hossack, J.R., 1968, Pebble deformation and thrusting in the Bygdin area (southern Norway). Tectonophysics 5, 315-339.

Dunnet, D., 1969, A technique of finite strain analysis using elliptical particles. Tectonophysics 7, 117-136.

Lisle, R.J., 1979, Strain analysis using pebbles; the influence of initial pebble shape. Tectonophysics 60, 263-277.

Lisle, R.J., 1985, Geological strain analysis; a manual for the R_f/Φ technique. Pergamon Press, Oxford.

Onasch, C.M., 1984, Application of the R_f/Φ technique to elliptical markers deformed by pressure-solution, Tectonophysics 110, 167-165.

Paterson, S.R., and Yu, H., 1994, Primary fabric ellipsoids in sandstones; implications for depositional processes and strain analysis. Journal of Structural Geology 16, 505-517.

Ramsay, J.G., 1967, Folding and fracturing of rocks, McGraw Hill, New York, 568 p.

Ramsay, J.G., and Huber, M.I., 1983, Strain analysis, Techniques of modern structural geology, Volume 1. Academic Press, London 307 p.

Treagus, S.H., and Treagus, J.E., 2002, Studies of strain and rheology of conglomerates. Journal of Structural Geology 24, 1541-1567.

Yamaji, A., 2005, Finite tectonic strain and its error, as estimated from elliptical objects with a class of initial preferred orientations. Journal of Structural Geology 27, 2030-2042.

Figure and Table Captions

Figure 1. Screen captures of the entire program window. **A.** Individual ellipses can be drawn in editing mode with a wide variety of colors. **B.** Photographs (up to 700 by 700 pixels) of deformed objects, such as these quartz pebbles, are imported in the display window for tracing ellipses as shown in blue.

Figure 2. Screen captures of the display window and Cartesian and polar R_f-Φ plots. **A.** Undeformed (axial ratio of strain ellipse, Rs = 1) array of color-coded ellipses. **B.** Plot of R_f vs. Φ for the unstrained configuration of ellipses shown in A. **C.** Polar plot of $\ln(R_f)$ vs. 2Φ for the unstrained configuration of ellipses shown in A. **D.** Ellipses shown in A after vertical shortening by pure shear such that the axial ratio of the strain ellipse, Rs, is equal to 1.4. **E.** Plot of R_f vs. Φ for the ellipses shown in D. **F.** Polar plot of $\ln(R_f)$ vs. 2Φ for the ellipses shown in D. **G.** Ellipses shown in A after vertical shortening by pure shear such that the axial ratio of the strain ellipse, Rs, is equal to 3. **H.** Plot of R_f vs. Φ for the ellipses shown in G. **I.** Polar plot of $\ln(R_f)$ vs. 2Φ for the ellipses shown in G. Note that the display screens in D and G were rescaled to show all the pebbles after deformation. R_{fmax} and R_{fmin} in E and H are the maximum and minimum axial ratios used to find the values of the strain ellipse, R_s, and maximum initial axial ratio, R_{imax}, in Eqs. (1) through (4).

Figure 3. Screen captures of the entire program window and the Cartesian and polar R_f-Φ plots. **A.** Photograph (700x700 pixels) of deformed quartz-pebble conglomerate imported as background image. **B.** Plot of R_f vs. Φ of the deformed pebbles in A. **C.** Polar plot of $\ln(R_f)$ vs. 2Φ of the deformed pebbles in A. **D.** Pebble outlines after 9^o of counter-clockwise rigid rotation. **E.** Plot of R_f vs. Φ of the pebbles after 9^o of counter-clockwise rigid rotation. **F.** Polar plot of $\ln(R_f)$ vs. 2Φ of the pebbles after 9^o of counter-clockwise rigid rotation. **G.** Pebble outlines after horizontal shortening by pure shear such that the axial ratio of the inverse strain ellipse is equal to 3.7. Note that the display screen in G was rescaled to show all the pebbles after deformation. **H.** Plot of R_f vs. Φ of the

pebbles after horizontal shortening by pure shear such that the axial ratio of the inverse strain ellipse is equal to 3.7. The inverse strain value was determined by trial and error to create the most dispersed distribution of points over the entire range of Φ values to simulate an initially random distribution of long axis orientations. **I.** Polar plot of $\ln(R_f)$ vs. 2Φ of the pebbles after horizontal shortening by pure shear such that the axial ratio of the inverse strain ellipse is equal to 3.7. The inverse strain value was determined by trial and error to create a radial distribution of points centered at the origin to simulate an initially random distribution of long axis orientations.

Table 1. Abbreviations used in text and figures.

Table 2. Abbreviated explanation of GeoShear command buttons to illustrate available functions.

Figure 1

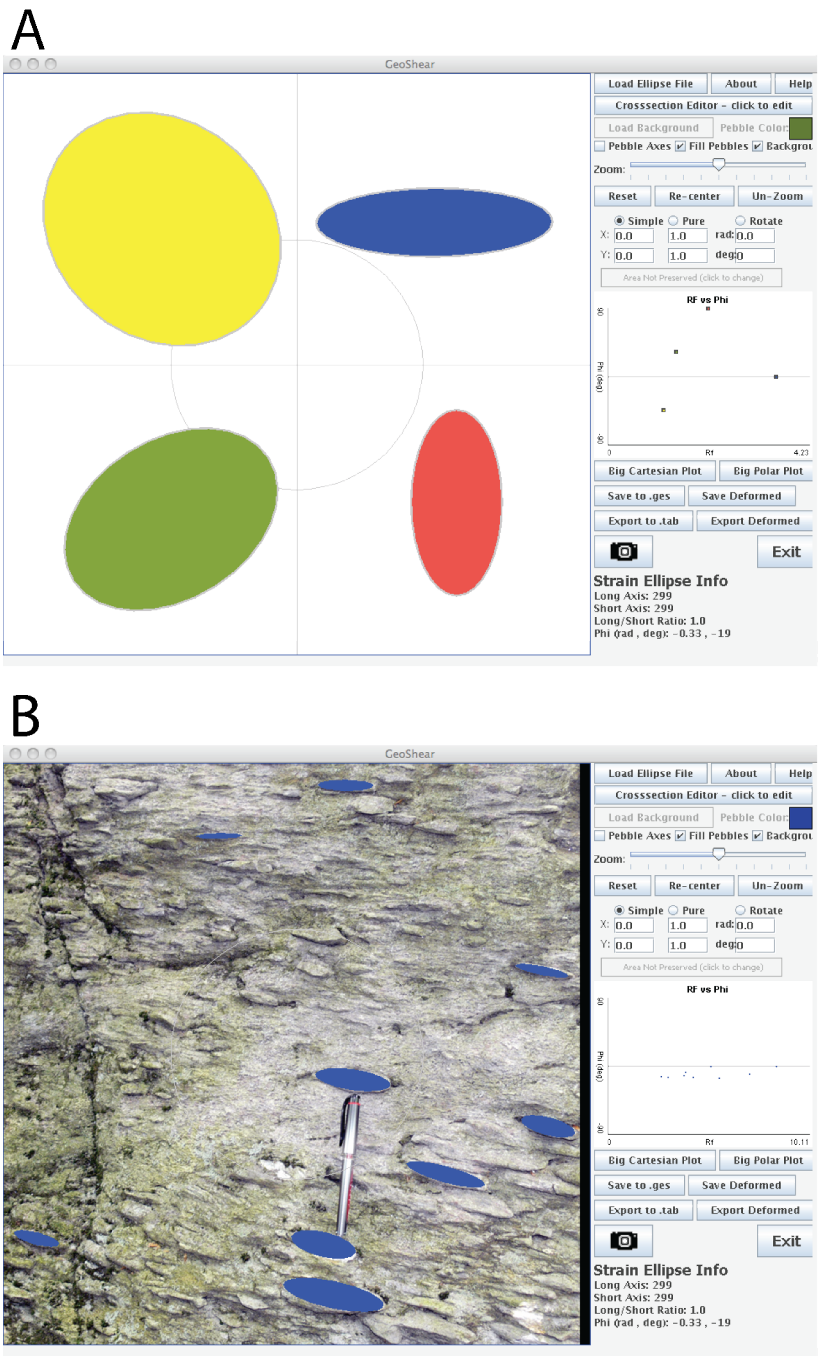

Figure 1.

Figure 2

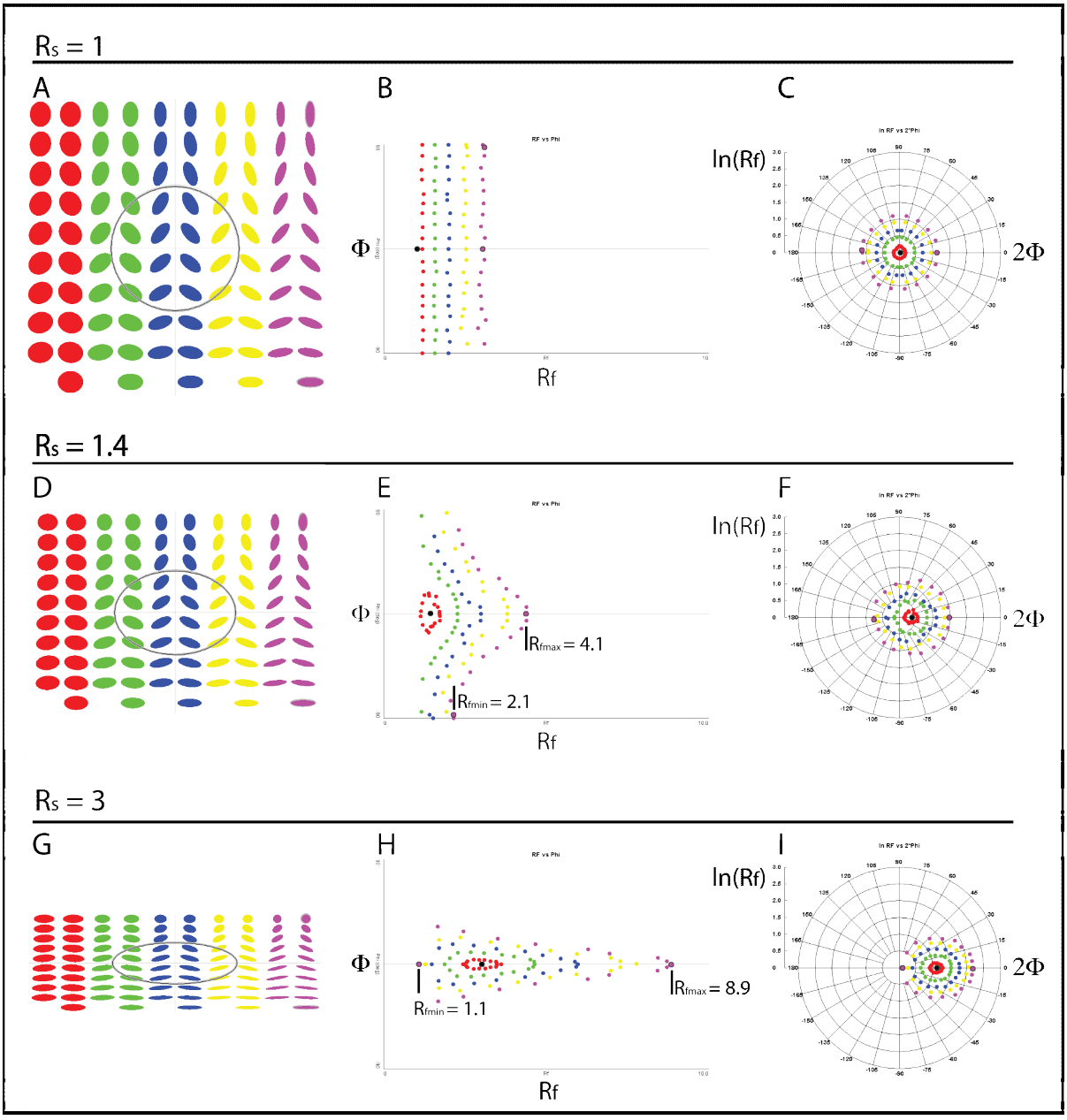

Figure 2.

Figure 3

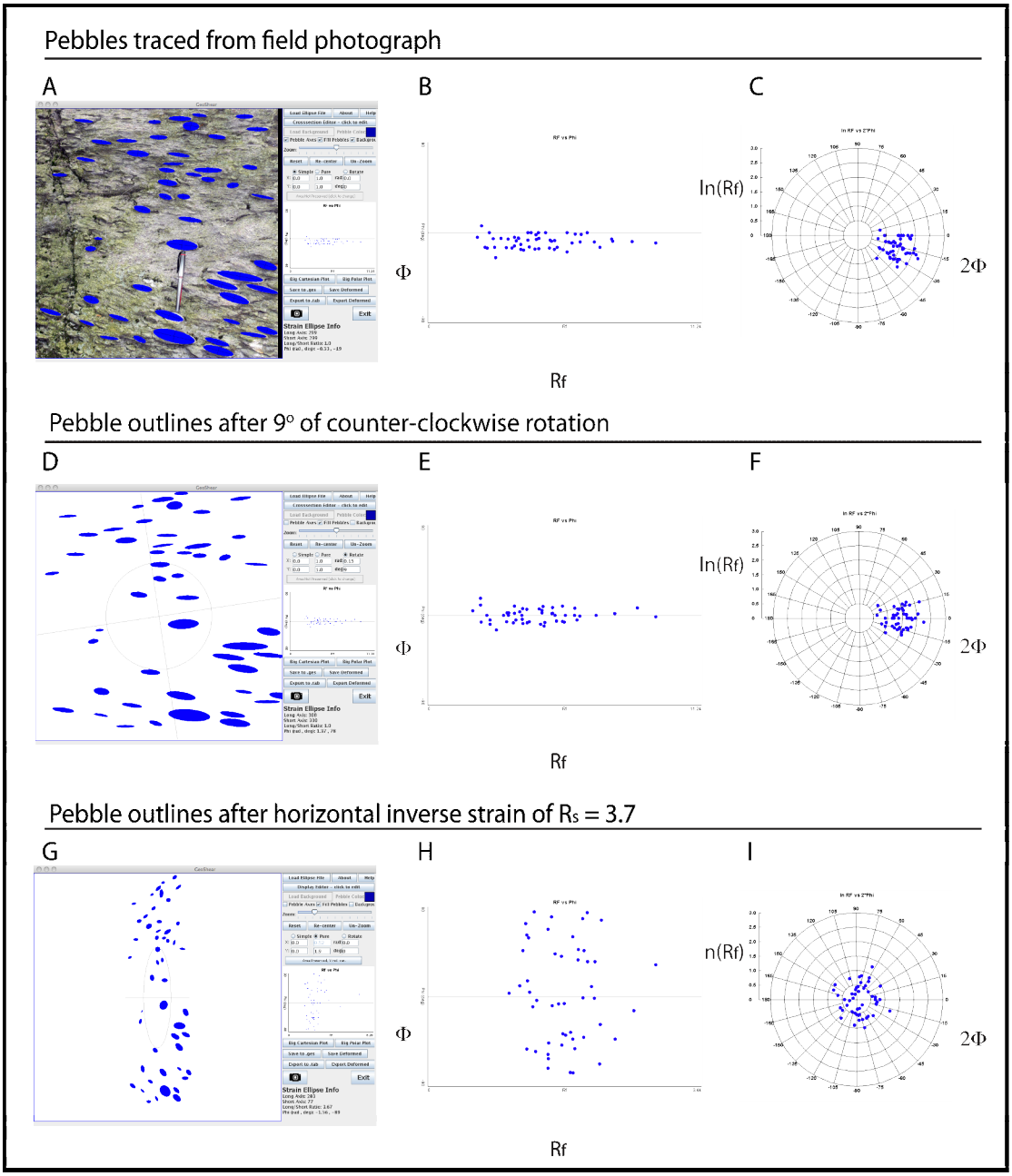

Figure 3.

Table

Table 1. Abbreviations used in text and figures.

Φ	The angle between an arbitrary reference line and the long axis of an ellipse. Range: -90^{o} to 90^{o}.
R_f	The final axial ratio (long axis/short axis) of any arbitrary elliptical object.
R_{fmax}	The maximum final axial ratio of all the elliptical objects.
R_{fmin}	The minimum final axial ratio of all the elliptical objects.
R_i	The initial axial ratio of any arbitrary elliptical object.
R_{imax}	The maximum initial axial ratio of all the elliptical objects.
R_s	The axial ratio of the strain ellipse (long axis/short axis).

Table 2. Abbreviated explanation of GeoShear command buttons to illustrate available functions.

Command	Function
Load Ellipse File	Loads an existing ellipse data file that contains shape, orientation position, and color information.
Help	Brings up the help window.
About	Displays information about this program.
Display Editor	Allows you to draw elliptical objects with the mouse, load a background image, and trace ellipses from a background image.
Load Background	Loads an image background for tracing elliptical objects.
Pebble Color	Double-click on the box to change the color. Change the color of all selected pebbles by ALT-clicking on the color box.
Pebble Axes	Toggles between showing and hiding long and short axes of elliptical objects.
Fill Pebbles	Toggles between filled and outlined pebbles.
Background	Toggles between showing and hiding the loaded background.
Zoom	Change the magnification of the cross section from 20% to 500%.
Reset	Removes all deformation, positioning, and magnification changes.
Re-Center Display	Re-centers the display but preserves deformation. The display may be moved off center by holding down the ALT key and dragging in the display area.
Un-Zoom	Returns display to the default magnification of 100%.
Simple shear	Constrains deformation to be by simple shear. Click and drag in the display to deform elliptical objects. You can also type in exact values for simple shear in the horizontal and/or vertical directions in the rectangles below the radio button.
Pure shear	Constrains deformation to be by pure shear. Click and drag in the display to deform elliptical objects. You can also type in exact values for extension in the horizontal and vertical directions in the rectangles below the radio button.
Area Not Preserved (click to change)	Toggles between three options. The first allows area to change during pure shear. **Area Preserved, Y Ind. Var.** lets you specify the vertical extension and adjusts horizontal extension to preserve area. **Area Preserved, X Ind. Var.** lets you specify the horizontal extension and adjusts vertical extension to preserve area.
Lock in current deformation	Used when switching from simple shear, pure shear, or rotation, to another deformation mode. Resets frame of reference.
Rotate	Constrains deformation to be by rotation. Click and drag in the display to rotate objects. You can also type in exact rotation angles as either degree or radians.
Big Cartesian Plot	A larger Cartesian Rf vs. Φ plot opens up in a new, re-sizeable window if this button is pressed.
Big Polar Plot	A polar plot of ln(Rf) vs. 2(Φ) opens up in a new, re-sizeable window if this button is pressed.
Save to ges.	Save the starting display to a file. The file retains the background and all the elliptical objects, but not subsequent deformation or other display changes.
Save Deformed	Save a deformed display, but not the original shapes.
Export to tab.	Saves the undeformed pebble information to a tab-delimited file.
Export Deformed	Saves the deformed pebble information to a tab-delimited file.
Camera	Take a snapshot of the current display. It will capture whatever is in the display area as a PNG, BMP, or JPG image.
Exit	Exits the program without saving anything.
Strain Ellipse Info	This area displays information about the strain ellipse (the grey circle in the center that you can see when no background is displayed).